

Electroplated reticulated vitreous carbon current collectors for lead–acid batteries: opportunities and challenges

Elod Gyenge^{a,*}, Joey Jung^b, Basanta Mahato^c

^aDepartment of Chemical and Biological Engineering, The University of British Columbia, 2216 Main Mall, Vancouver, Canada V6T 1Z4

^bBC Research Inc., Power Technology Research and Development Laboratory, 3650 Wesbrook Mall, Vancouver, BC, Canada V6S 2L2

^cBattery Consultation Services, 18826 Academy Circle, Huntington Beach, CA 92648, USA

Abstract

Reticulated, open-cell structures based on vitreous carbon substrates electroplated with a Pb–Sn (1 wt.%) alloy were investigated as current collectors for lead–acid batteries. Scanning and backscattered electron microscopy, cyclic voltammetry, anodic polarization and flooded 2 V single-cell battery testing was employed to characterize the performance of the proposed collectors. A battery equipped with pasted electroplated reticulated vitreous carbon (RVC) electrodes of 137 cm² geometric area, at the time of manuscript submission, completed 500 cycles and over 1500 h of continuous operation. The cycling involved discharges at 63 A kg_{PAM}⁻¹ corresponding to a nominal 0.75 h rate and a positive active mass (PAM) utilization efficiency of 21%. The charging protocol was composed of two voltage limited (i.e. 2.6 V/cell), constant current steps of 35 and 9.5 A kg_{PAM}⁻¹, respectively, with a total duration of about 2 h. The charge factor was 1.05–1.15. The observed cycling behavior in conjunction with the versatility of electrodeposition to produce application-dependent optimized lead alloy coating thickness and composition shows promise for the development of lead–acid batteries using electroplated reticulated vitreous carbon collectors.

© 2002 Elsevier Science B.V. All rights reserved.

Keywords: Lead–acid battery; Current collector; Reticulated vitreous carbon; Electroplating

1. Introduction

The utilization efficiency of the active mass and the cycle life of the lead–acid battery are determined by the complex phenomena occurring at the current collector—active material—electrolyte interface. It has been recognized that the design of the current collector structure, by its influence on the α and γ factors characterizing the battery plates, has an important role with regard to active mass utilization and cycle life [1]. For cast book-mould collectors the α factor (i.e. ratio of collector to plate weight, $g_{\text{COL}} g_{\text{PLATE}}^{-1}$) is typically about 0.5. The γ factor (i.e. ratio of positive active mass (PAM) to collector surface area, $g_{\text{PAM}} \text{cm}_{\text{COL}}^{-2}$) typically ranges between 1.6–1.8 for tubular and 2–2.5 for book-mould SLI plates, respectively. In order to increase the utilization efficiency of the positive active mass, the latest trend is to design plates with low γ factors (e.g. $\gamma < 1 g_{\text{PAM}} \text{cm}_{\text{COL}}^{-2}$ [1]). However, there seems to be an optimum γ value with respect to both electrochemical performance and mechanical integrity of the plates affecting

battery cycle life (e.g. softening and shedding of the active mass). There is no clear indication in the literature regarding the determination of the optimal γ for a particular lead–acid battery type. It is likely that a combination of mathematical modeling and experimental studies could lead to the identification of the optimum plate γ factor for a certain battery type and intended application.

Recently, it has been shown that cast reticulated, open-cell current collector structures, characterized by a specific surface area of 14 cm² cm⁻³, yielded battery plate γ factors as low as 0.3 $g_{\text{PAM}} \text{cm}_{\text{COL}}^{-2}$ and PAM utilization efficiencies up to 50% higher than typical book-mould grids [2]. At 3 h discharge rate the capacity of a single-cell battery with cast reticulated collectors was 101 Ah kg_{PAM}⁻¹, while a test cell equipped with radial design book-mould grids yielded only 66 Ah kg_{PAM}⁻¹.

A further advancement in the area of lead–acid battery collectors is the use of structures based on lightweight reticulated substrates such as reticulated vitreous carbon (RVC). The latter material offers superior manufacturing control and versatility as compared to cast reticulated lead [3]. The combination of high specific surface area (e.g. >10 cm² cm⁻³) and optimal use of lead or lead alloy could

* Corresponding author. Tel.: +1-604-822-3217; fax: +1-604-822-6003.
E-mail address: egypte@chml.ubc.ca (E. Gyenge).

lead to significant improvement of the battery specific energy and energy density.

There are only a few reports on the use of carbon materials in lead–acid battery collectors. Studies on graphitized carbon fabrics revealed that the bare carbon material could be only useful as a negative collector, since under conditions relevant to the functioning of the positive battery electrode significant changes in surface functional groups were observed leading to deterioration of performance and long-term stability [4].

Cyclic voltammetry studies of electrodeposited Pb and PbO₂ on RVC showed that the carbon substrate had virtually no effect on the apparent electrochemical behavior of either Pb or PbO₂. On the other hand, the presence of a Pt layer in between RVC and electrodeposited Pb diminished the peak current density for PbO₂ reduction after the first voltammetric sweep. Therefore, it was concluded that bare RVC could serve as an effective substrate material for lead–acid battery current collectors [5,6].

It must be noted, however, that the above conclusion was reached based solely on cyclic voltammetry experiments. Therefore, caution must be exercised when extrapolating these observations to the long-term functioning of an operational lead–acid battery.

A Planté type (i.e. unpasted plates) flooded, lead–acid battery cell was assembled and cycled using small Pb electrodeposited carbon rods of 0.125 cm² exposed area [7,8]. On the positive electrode PbO₂ was formed by electro-oxidation of the electrodeposited Pb layer. It was found that the capacity of the cell increased with both deposition time (i.e. amount of deposited Pb) and cycling. Furthermore, the cell capacity was limited by the negative electrode, which was attributed to the slow development of a ‘spongy’ negative active mass. The cycling characteristics of the positive electrode (i.e. PbO₂/PbSO₄) was strongly dependent on the H₂SO₄ concentration. At 4 M acid concentration (estimated relative density 1.235 [9]) the contact between PbO₂ and carbon substrate was poor, causing the shedding of the PAM. In more dilute acid, 1–2.5 M (estimated relative density 1.065–1.150 [9]) a good adhesion between PbO₂ and the carbon substrate was observed [8].

The goal of the present study was two-fold. First, to develop and electrochemically characterize Pb-alloy electrodeposited RVC collectors of geometric area suitable for use in realistic lead–acid batteries (e.g. geometric area >100 cm²). Second, to test the cycling performance of positive-limited flooded 2 V single-cell batteries equipped with pasted electrodeposited RVC electrodes.

2. Experimental

Table 1 presents selected physical characteristics of the reticulated vitreous carbon (ERG Inc.) used in the present work. RVC slabs of 12.7 cm × 12.7 cm × 0.35 cm (height × width × thickness) were galvanostatically plated with a

Table 1
Selected physical characteristics of the reticulated vitreous carbon

Property	Value	Reference
Number of pores per cm (ppc)	12	[10]
Specific surface area (cm ² cm ⁻³)	18	[10]
Bulk density (g cm ⁻³)	0.048	[10]
Porosity	0.78	[11]
Bulk electronic conductivity of the reticulated matrix (S cm ⁻¹)	1.2	[11]
Electronic conductivity of the carbon ligament (S cm ⁻¹)	200	[10]

Pb–Sn (1 wt.%) alloy, using a fluoroborate bath [12,13]. Fig. 1a and b show SEM images of the open-cell structure for the bare RVC and the electroplated positive reticulated collector.

Typically a coating thickness of 200–300 μm was applied for the positive and 80–120 μm for the negative collector, respectively. Thus, the overall weight of the collectors was designed such that to balance the cycle life requirements for the flooded battery (i.e. thick coating on the positive grid

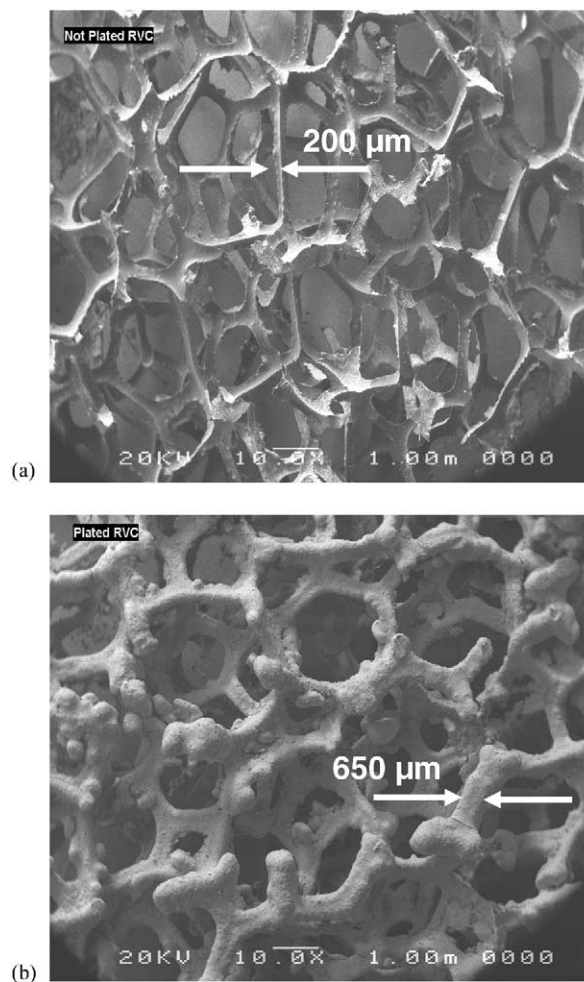


Fig. 1. Scanning electron microscopy images of the reticulated open-cell structure: (a) bare RVC; (b) electroplated RVC for the positive collector.

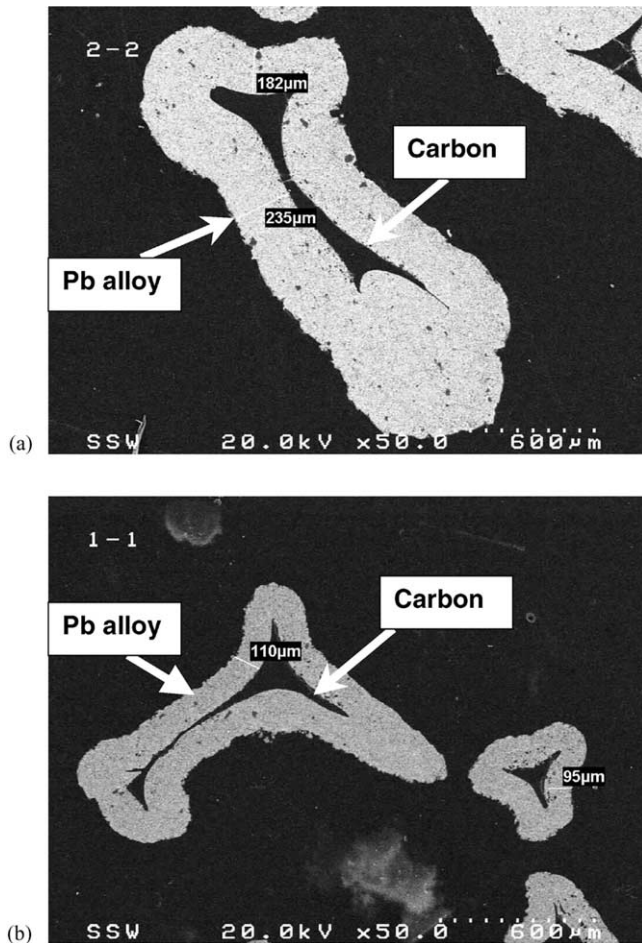


Fig. 2. Backscattered electron microscopy of representative cross-sections for electroplated RVC: (a) positive collector; (b) negative collector.

exposed to corrosion) and battery weight reduction (i.e. thin coating on the negative grid).

Backscattered electron microscopy of representative cross-sections for the positive and negative collectors

(Fig. 2a and b, respectively) indicate a good contact between the carbon ligament and the Pb–Sn deposit. Based on Fig. 2, the coating can be considered as dense, with only a few pinholes present with diameters between approximately 0.5 and 5 μm .

Cyclic voltammetry and corrosion experiments were performed using an AMEL 2055 high-power potentiostat connected to a Pentium III PC via a PowerLab/4SP data acquisition board and Echem[®] 1.51 software (AD Instruments). The electrolyte was 600 ml of H_2SO_4 with a relative density of 1.3. Reticulated test coupons (both bare and plated RVC) with a geometric area between 16 and 19 cm^2 were used. The thickness of the bare RVC coupons was 0.3 cm, while the plated samples had an average thickness of 0.47 cm. The counter electrode was either a graphite rod or a cylindrical Pt mesh. A mercurous sulfate electrode (MSE) filled with H_2SO_4 of 1.3 relative density and connected through a Luggin capillary served as reference.

To gain insights into the corrosion behavior of the electrodeposited reticulated structure, constant anodic polarization experiments were performed at 295 and 313 K, respectively. The test coupons, immersed in H_2SO_4 of 1.3 relative density, were subjected to three different potentials, 1.25, 1.35 and 1.45 V versus MSE. The open-circuit potential for the PbO_2 electrode was 1.18 V versus MSE. The duration of exposure at each anode potential was 13 days. After exposure, the coupon dimensions were measured to determine the three-dimensional growth due to corrosion. The weight losses of the coupons were obtained following chemical stripping of the oxidation products in alkaline hydrazine–mannitol solution at 70 $^\circ\text{C}$ for about 30–60 s.

For battery testing, 2 V single-cell units were assembled using two negatives and one positive plate with electrodeposited RVC collectors. Fig. 3 shows a typical collector design with a size of 11.8 cm \times 11.6 cm (height \times width), geometric area 137 cm^2 . The thickness was 0.54 cm for the positive and 0.33 cm for the negative plate, respectively.

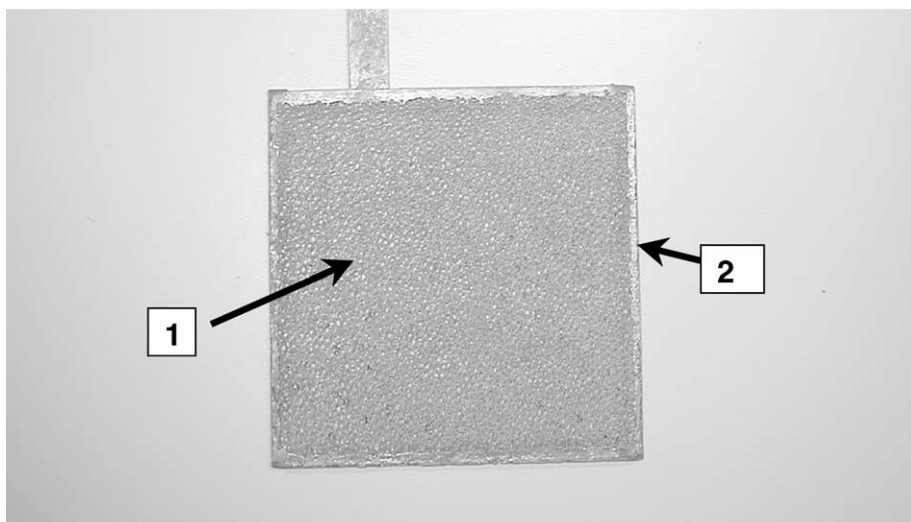


Fig. 3. Electrodeposited RVC current collector for lead-acid batteries: (1) reticulated mesh; (2) frame and tab.

Table 2
Typical component weight percentages for the reticulated collectors

Component	Positive collector (wt.%)	Negative collector (wt.%)
RVC substrate	2	3
Lead alloy coating	53	65
Frame and tab	45	32

Table 2 gives the weight percentages of the various collector components (e.g. substrate, coating and frame with tab). The weight of the RVC substrate accounts for only 2–3% of the total collector weight (Table 2).

The collectors were manually pasted using a PbO–PbSO₄ based paste from an industrial source. The pasted plates were cured at 80 °C for 24 h at a relative humidity of 90–100. Forming was performed in 1.115 relative density H₂SO₄ with a charge of 520 Ah kg_{PAM}⁻¹.

Table 3 shows the apparent current collector density ρ (Eq. (1)), and the plate design parameters α (Eq. (2)) and γ (Eq. (3)) for the formed reticulated battery;

$$\rho = \frac{m_{\text{COL}}}{A_{\text{COL}} \tau_{\text{COL}}} \quad (\text{g}_{\text{COL}} \text{cm}_{\text{COL}}^{-3}), \quad (1)$$

$$\alpha = \frac{m_{\text{COL}}}{m_{\text{COL}} + m_{\text{AM}}} \quad (\text{g}_{\text{COL}} \text{g}_{\text{PLATE}}^{-1}), \quad (2)$$

and

$$\gamma = \frac{m_{\text{AM}}}{a_{\text{COL}} A_{\text{COL}} \tau_{\text{COL}}} \quad (\text{g}_{\text{AM}} \text{cm}_{\text{COL}}^{-2}). \quad (3)$$

where a_{COL} , A_{COL} , m_{COL} and τ_{COL} are the specific surface area (cm² cm⁻³), geometric area (cm²), weight (g) and thickness (cm) of the collector, respectively, while m_{AM} is the active mass (on either the positive or negative plate).

Table 3
The apparent collector density and plate design parameters for the electrodeposited RVC

Electrode	ρ (g _{COL} cm _{COL} ⁻³)	α (g _{COL} g _{PLATE} ⁻¹)	γ (g _{AM} cm _{COL} ⁻²)
Positive reticulated	2.0	0.64	0.09
Negative reticulated	1.3	0.38	0.13
Book-mould	3.1–5	0.47–0.60	0.66–1.23

Note: for comparison typical values for conventional book-mould collectors used in our laboratory, are also given.

As shown by Table 3, in the case of the reticulated collector ρ was at least 35% lower, whilst γ was reduced by more than order of magnitude as compared to a reference book-mould grid design. Furthermore, the α factor of the negative plate was also reduced by about 20–35%.

For battery cycling experiments, the electrolyte was H₂SO₄ with an initial relative density of 1.300 at 295 K. The discharge cut-off voltage was 1.63 V. Battery testing was performed using UBA4 battery analyzers and associated software (Vencon Technologies Inc.) controlled by a Pentium III PC. The maximum current output per channel was 2 A for charge and 2.5 A for discharge, respectively.

3. Results and discussion

The cyclic voltammogram of the bare RVC was recorded in both anodic and cathodic regions, respectively. Fig. 4 shows the voltammetric behavior of RVC over 50 cycles between 0.8 and 1.45 V at a sweep rate of 1 mV s⁻¹. An oxidation current was measured starting at a potential of approximately 1.05 V. During 50 cycles, for a potential of 1.3 V the anodic current density was <0.1 mA cm⁻² while at

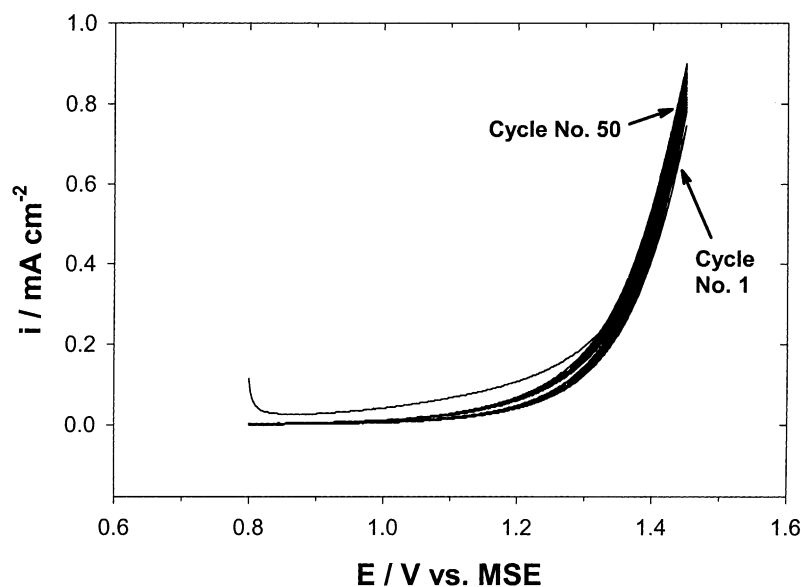


Fig. 4. Cyclic voltammogram of bare RVC between 0.8 and 1.45 V vs. MSE. Electrolyte: 1.3 relative density H₂SO₄. Temperature: 295 K. Sweep rate: 1 mV s⁻¹.

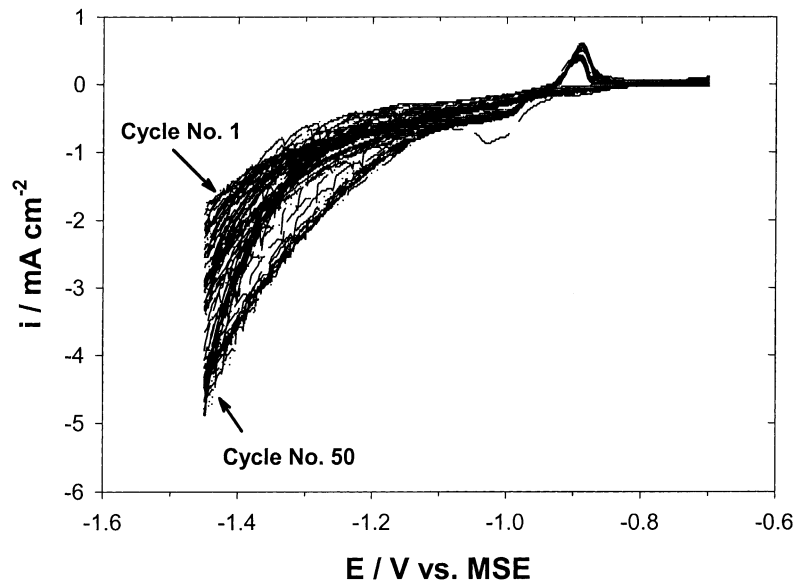


Fig. 5. Cyclic voltammogram of bare RVC between -0.7 and -1.45 V vs. MSE. Electrolyte: 1.3 relative density H_2SO_4 . Temperature: 295 K. Sweep rate: 1 mV s^{-1} .

1.45 V the current density increased to 0.9 mA cm^{-2} (Fig. 4). Under comparable conditions various graphitized carbon fabric materials showed much larger anodic current densities, in the range of $10\text{--}100 \text{ mA cm}^{-2}$ [6]. One might, therefore, conclude that vitreous carbon is electrochemically more stable under the operating conditions of the positive electrode in lead–acid batteries.

The X-ray photoelectron spectroscopy (XPS) spectrum of the RVC sample was recorded both before and after fifty anodic cycles. It was found that the oxygen content of the sample doubled during anodic cycling due to the formation of $-\text{C}=\text{O}$ and $-\text{COOH}$ surface functional groups. However, after

50 polarization cycles the mechanical integrity of the RVC skeleton was satisfactory. From the point of view of battery operation, therefore, one has to take into account the fact that at potentials relevant to the charging of the positive electrode the RVC substrate undergoes oxidation if H_2SO_4 penetrates through the Pb alloy coating. It is plausible to assume that prolonged exposure and oxidation of the carbon matrix could eventually lead to the weakening of the collector structure.

The voltammogram of the bare RVC in the cathodic region, between -0.7 and -1.45 V (Fig. 5), indicates that the onset of H_2 evolution occurs at about -0.95 V. For cycle number 50, at a potential of -1.4 V, the cathodic current

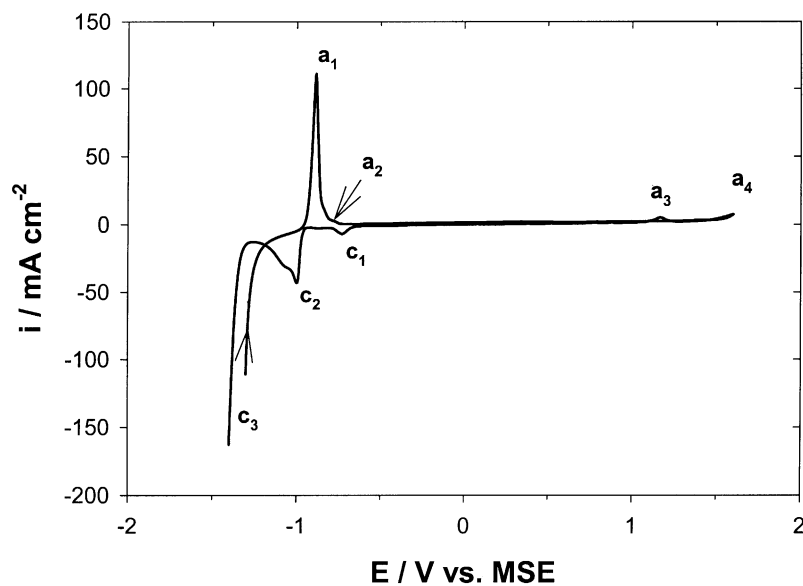


Fig. 6. Cyclic voltammogram of the Pb–Sn (1 wt.%) electrodeposited RVC. Electrolyte: 1.3 relative density H_2SO_4 . Temperature: 295 K. Sweep rate: 5 mV s^{-1} .

density was 5 mA cm^{-2} . Thus, at potentials representative for negative plate charging, H_2 evolution occurs on the RVC substrate if exposed to acid.

The above experimental results indicate clearly that in order to minimize both the oxidation of the RVC matrix and H_2 evolution at the carbon/lead interface, a dense and pin-hole-free lead alloy must be electrodeposited (see Fig. 2a and b).

Fig. 6 shows the cyclic voltammogram of the Pb–Sn (1 wt.%) electrodeposited RVC recorded at a sweep rate of 5 mV s^{-1} for potentials between -1.4 and 1.6 V . The voltammogram shows the characteristic electrochemical features of Pb–Sn alloys [14,15]. On the anodic scan, the peak at -0.89 V corresponding to the oxidation of Pb to PbSO_4 (a_1 , Fig. 6) is followed by a small shoulder-like wave at -0.78 V , given by the oxidation of Sn (1 wt.% in the alloy) to SnSO_4 (a_2 , Fig. 6) [15].

Further on the anodic scan, at a potential of 1.6 V corresponding to O_2 evolution and PbO_2 formation the current density was only about 10 mA cm^{-2} (a_4 , Fig. 6). For comparison, a reticulated structure without Sn present gave about an order of magnitude higher current density at a potential of 1.6 V [2]. Thus, the presence of Sn increases the overpotential for O_2 evolution and PbO_2 formation [14].

Scanning in the cathodic direction, first an oxidation peak (a_3) was obtained at 1.2 V . The presence of this anodic peak was previously described in the literature [5]. It was attributed to either H_2O oxidation by PbO_2 [16] or to cracking associated with molar volume increase when PbO_2 is reduced to PbSO_4 [17]. Since in the present case, during one sweep, no cathodic peak was obtained corresponding to PbO_2 reduction (usually observed at about 1.1 V [2]) the water oxidation hypothesis seems more plausible.

Further on the cathodic scan, due to the presence of Sn in the alloy, the PbO reduction peak potential (c_1) was obtained at a more positive potential, i.e. -0.74 V (Fig. 6). Typically, in the absence of Sn the PbO reduction peak potential was around -0.88 V [2]. The shift of PbO reduction to more positive potentials is part of the well-documented ‘tin effect’ for lead–acid battery current collectors manufactured from Sn containing Pb alloys [14,18].

At more negative potentials, (i.e. $\leq -1 \text{ V}$ versus MSE) two electrode reactions were observed: reduction of PbSO_4 to Pb (c_2 , Fig. 6, peak potential -1 V) and H_2 evolution (c_3 , at potentials $< -1.2 \text{ V}$).

Fig. 7 shows the weight losses of the three-dimensional reticulated coupons (on exposed geometric surface area basis) after 13 days of anodic polarization at each of the investigated potentials (1.25 , 1.35 and 1.45 V , respectively). Experiments were performed at both 295 and 313 K .

The lowest corrosion rate was observed at 295 K for an anode potential of 1.35 V . In this case the weight loss was about 2 mg cm^{-2} (Fig. 7). The effect of temperature was most pronounced at higher anodic potentials. For instance, at 1.25 V increasing the temperature from 295 to 313 K produced only a slight increase of weight loss from 2.7 to 3.5 mg cm^{-2} . At 1.45 V on the other hand, the temperature increase produced approximately an eight times higher weight loss, 28 versus 3.7 mg cm^{-2} (Fig. 7). Unfortunately, there is no literature data on reticulated collector corrosion to compare the present data with. However, for an expanded grid made of ternary Pb–(0.088 wt.%) Ca–(0.34 wt.%) Sn alloy, a 4 mg cm^{-2} weight loss was reported after 14 days of exposure at 1.36 V and 323 K in H_2SO_4 of 1.28 relative density [19]. Further studies by a combination of electrochemical and surface science methods are required to fully

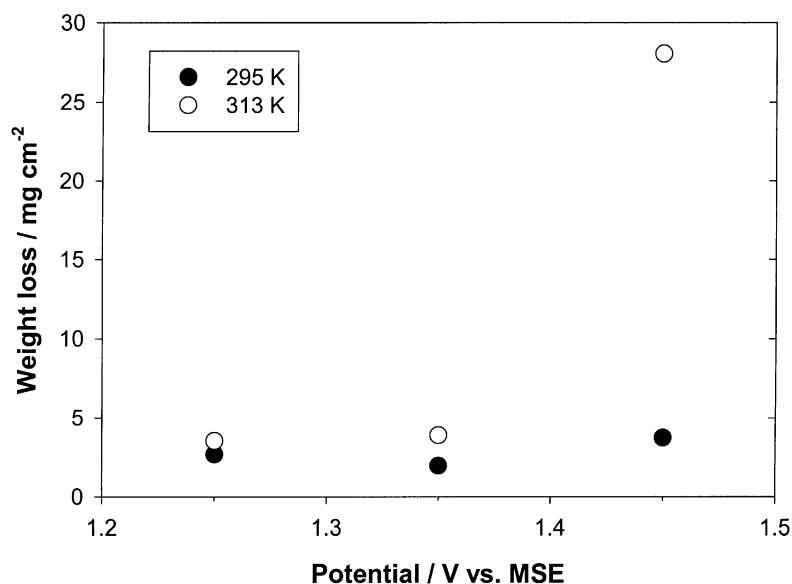


Fig. 7. Anodic polarization of Pb–Sn (1 wt.%) electrodeposited RVC. Duration of exposure at each potential value: 13 days. Electrolyte: 1.3 relative density H_2SO_4 . Legend: (●) 295 K , (○) 313 K .

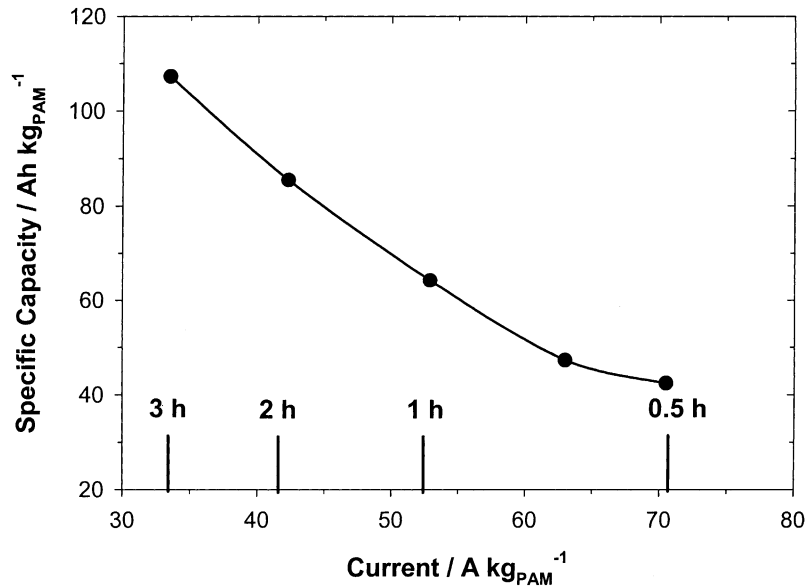


Fig. 8. Peukert diagram for the positive electrodeposited RVC collector in a flooded battery.

understand the corrosion behavior of the novel electrodeposited RVC current collectors.

The nominal capacities (Peukert diagram) at discharge rates between 0.5 and 3 h for the positive-limited reticulated battery are shown by Fig. 8. At a discharge current of $33.5 \text{ A kg}_{\text{PAM}}^{-1}$, corresponding to a discharge rate of 3 h, the PAM utilization efficiency on the electrodeposited reticulated collector was 48% (specific capacity $107 \text{ Ah kg}_{\text{PAM}}^{-1}$, Fig. 8). Discharging the reticulated battery at 1 h rate ($53 \text{ A kg}_{\text{PAM}}^{-1}$) yielded a PAM utilization of 29% corresponding to a capacity of $64 \text{ Ah kg}_{\text{PAM}}^{-1}$ (Fig. 8).

A test cell composed of one positive and two negative reticulated electrodes was subjected to long-term cycling.

Each cycle comprised of a discharge at $63 \text{ A kg}_{\text{PAM}}^{-1}$ (nominal utilization efficiency 21% and 0.75 h rate) followed by a two-step constant current charge returning between 105 and 115% charge compared to the previous discharge. The voltage limited (2.6 V/cell) constant current charging steps were as follows; step 1: $35 \text{ A kg}_{\text{PAM}}^{-1}$ and step 2: $9.5 \text{ A kg}_{\text{PAM}}^{-1}$. The total duration of one charge–discharge cycle was about 2.8 h.

Under the above cycling conditions, at the time of manuscript submission, the electrodeposited RVC battery completed 500 cycles corresponding to over 1500 h of continuous operation (Fig. 9). For the 500th cycle the capacity was $54.3 \text{ Ah kg}_{\text{PAM}}^{-1}$ (i.e. about 13% higher than the nominal value). The cycling test is continuing.

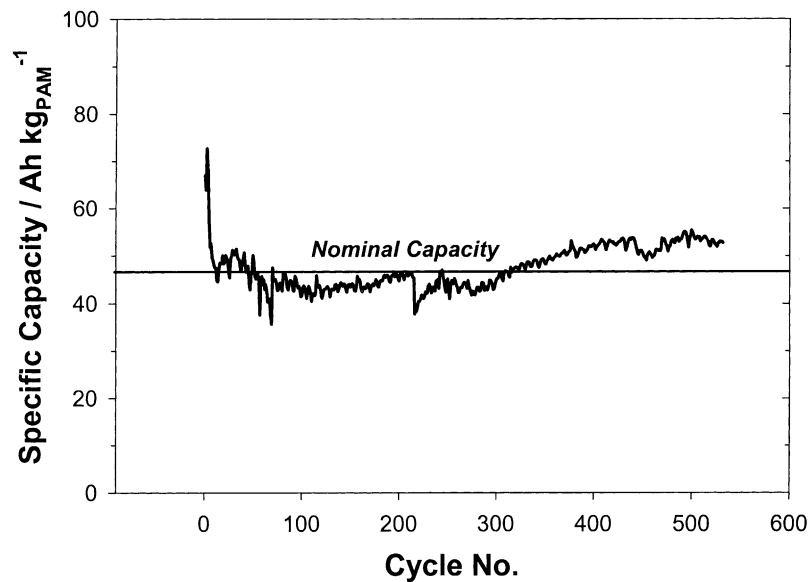


Fig. 9. Cycling performance of a positive limited flooded lead–acid battery equipped with electrodeposited RVC current collectors. Nominal capacity: $48 \text{ Ah kg}_{\text{PAM}}^{-1}$ (21% utilization efficiency). Discharge current: $63 \text{ A kg}_{\text{PAM}}^{-1}$.

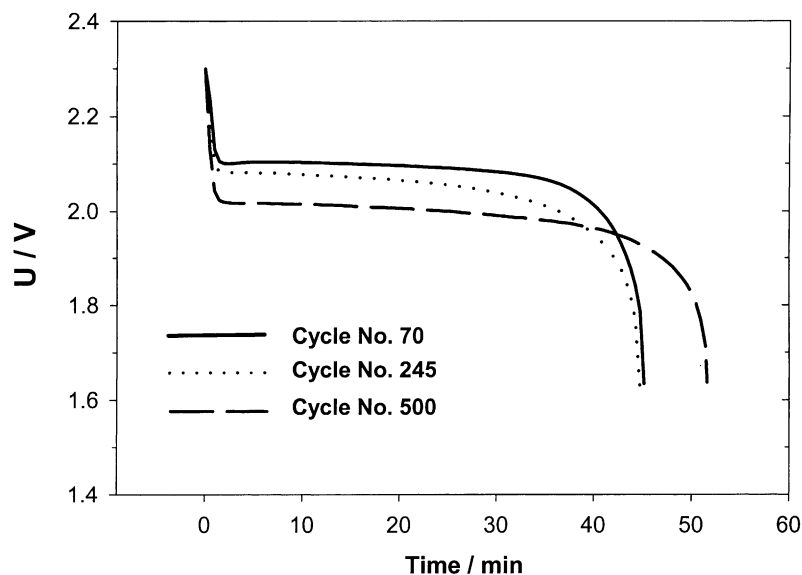


Fig. 10. Voltage profile of the electrodeposited RVC battery as a function of cycling. Discharge current: $63 \text{ A kg}_{\text{PAM}}^{-1}$.

Fig. 10 shows the battery voltage profile as a function of cycling. At cycle no. 245 the average discharge voltage was about 30 mV lower than for cycle no. 70, while for 500th cycle the average discharge voltage was still slightly above 2 V but approximately 90 mV lower than for cycle no. 70 (Fig. 10).

4. Conclusions

Pb–Sn (1 wt.%) electrodeposited reticulated vitreous carbon current collectors were developed, characterized and tested in 2 V single-cell flooded lead–acid batteries. The electrodeposition method offers the flexibility of producing collectors with a wide range of coating thickness, e.g. between 60 and 300 μm . Thus, the collector weight can be optimized as a function of the intended battery application and electrode polarity (i.e. a thin coating of up to 100 μm could be sufficient for the negative collector).

The measured anodic current densities for RVC in H_2SO_4 of 1.3 relative density were up to two orders of magnitude lower than the reported literature values for graphitized carbon fabric. This indicates the adequacy of vitreous carbon as a high specific surface area current collector substrate, under the operating conditions of lead–acid batteries.

Flooded, 2 V single-cell lead–acid batteries with electrodeposited RVC collectors were characterized by plate γ factors of about $\sim 0.1 \text{ g}_{\text{AM}} \text{ cm}_{\text{COL}}^{-2}$ and α factors of 0.38 (negative) and 0.64 (positive). At the time of manuscript preparation, 500 cycles corresponding to over 1500 h of continuous operation were completed, involving discharges at $63 \text{ A kg}_{\text{PAM}}^{-1}$, 0.75 h rate and nominal PAM utilization efficiency of 21%.

The promising cycle life result in conjunction with the improved PAM utilization efficiency due to low plate γ factor together with the application dependent and optimized

collector weight could lead to the development of high specific energy lead–acid batteries based on electrodeposited reticulated vitreous carbon electrodes.

References

- [1] D. Pavlov, J. Power Sources 53 (1995) 9.
- [2] E. Gyenge, J. Jung, S. Splinter, A. Snaper, J. Appl. Electrochem. 32 (2002) 287.
- [3] E. Gyenge, S. Splinter, J. Jung, A. Snaper, in: Proceedings of the 17th Annual Battery Conference on Applications and Advances. Long Beach, CA, 15–18 January 2002, Proc. IEEE 02TH8576 (2002) 19–24 (Ext. Abstr.).
- [4] A.V. Yuzhanina, N.A. Urison, Yu.A. Vetoshkin, T.D. Firsova, L.A. Maskovich, A.F. Kuteinkov, Russ. Electrochem. 26 (1990) 1127.
- [5] A. Czerwinski, M. Zelazowska, J. Electroanal. Chem. 410 (1996) 55.
- [6] A. Czerwinski, M. Zelazowska, J. Power Sources 64 (1997) 29.
- [7] K. Das, A. Mondal, J. Power Sources 55 (1995) 251.
- [8] K. Das, A. Mondal, J. Power Sources 89 (2000) 112.
- [9] D. Berndt, Maintenance-Free Batteries, 2nd ed., Research Studies Press Ltd., Taunton, England, 1997.
- [10] Reticulated Vitreous Carbon, Brochure, ERG Inc., Oakland, CA, 1997.
- [11] E. Gyenge, Ph.D. Thesis, University of British Columbia, Vancouver, Canada, 2001.
- [12] H.J. Wiesner, in: F.A. Lowenheim (Ed.), Lead in Modern Electroplating, Wiley, New York, 1974.
- [13] M. Jordan, Electrodeposition of Tin–Lead Alloys, in: M. Schlesinger, M. Paunovic (Eds.), Modern Electroplating, Wiley, New York, 2000.
- [14] I. Petersson, E. Ahlberg, J. Power Sources 91 (2000) 143.
- [15] M.N.C. Ijmoah, J. Appl. Electrochem. 18 (1988) 142.
- [16] J.G. Sunderland, J. Electroanal. Chem. 71 (1979) 341.
- [17] R.L. Deutscher, S. Fletcher, J.A. Hamilton, Electrochim. Acta 31 (1986) 585.
- [18] B. Culpin, A.F. Hollenkamp, D.A.J. Rand, J. Power Sources 38 (1992) 63.
- [19] E.M.L. Valeriote, J. Sklarchuk, M.S. Ho, Corrosion and growth of expanded grids for maintenance-free batteries, in: K.R. Bullock, D. Pavlov (Eds.), Advances in Lead–Acid Batteries, vol. 84–14. The Electrochemical Society, NJ, 1994, pp. 224–240.